

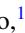





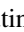










## Properties of the new $\alpha$ -decaying isotope $^{190}\text{At}$

H. Kokkonen <sup>1,\*</sup>, K. Auranen <sup>1</sup>, J. Uusitalo <sup>1</sup>, S. Eeckhaudt <sup>1</sup>, T. Grahn <sup>1</sup>, P. T. Greenlees <sup>1</sup>, P. Jones <sup>1,†</sup>, R. Julin <sup>1</sup>, S. Juutinen <sup>1</sup>, M. Leino <sup>1</sup>, A.-P. Leppänen <sup>1,‡</sup>, M. Nyman <sup>1,§</sup>, J. Pakarinen <sup>1</sup>, P. Rahkila <sup>1</sup>, J. Sarén <sup>1</sup>, C. Scholey <sup>1,||</sup>, J. Sorri <sup>1,¶</sup> and M. Venhart <sup>1,2</sup>

<sup>1</sup>Accelerator Laboratory, Department of Physics, University of Jyväskylä, FI-40014 Jyväskylä, Finland

<sup>2</sup>Institute of Physics, Slovak Academy of Sciences, SK-84511 Bratislava, Slovakia



(Received 20 March 2023; accepted 7 June 2023; published 20 June 2023)

The  $\alpha$  decay of a new isotope  $^{190}\text{At}$  has been studied via the  $^{109}\text{Ag}(^{84}\text{Sr}, 3n)^{190}\text{At}$  fusion-evaporation reaction by employing a gas-filled recoil separator. An  $\alpha$ -particle energy of 7750(20) keV and a half-life of  $1.0_{-0.4}^{+1.4}$  ms were measured. The measured decay properties correspond to an unhindered  $\alpha$  decay, suggesting the same spin and parity of ( $10^-$ ) as those of the final state of the decay. The systematics of the nearby nuclei and the predictions of selected atomic mass models were compared with the measured decay properties.

DOI: [10.1103/PhysRevC.107.064312](https://doi.org/10.1103/PhysRevC.107.064312)

### I. INTRODUCTION

Large-scale calculations, for example, the finite-range droplet model [1] and the Hartree-Fock-Bogoliubov (HFB) method based on the D1S Gogny effective nucleon-nucleon interaction [2,3], predict multitude of nuclear shapes in the  $Z > 82$ ,  $N \leq 126$  region. According to the models, nuclei near the closed  $N = 126$  neutron shell are nearly spherical in their ground state. Towards the proton dripline, nuclei are predicted to become slightly oblate deformed, and when approaching the neutron midshell  $N = 104$ , nuclei become strongly prolate deformed.

Experimental observations support the predicted shape evolution. For example, odd-mass astatine isotopes have been widely studied via  $\gamma$ -ray spectroscopy (see Refs. [4–7] and references therein). The  $9/2^-$  ( $\pi h_{9/2}$ ) ground states of astatine isotopes are observed to have a spherical or weakly oblate shape down to  $^{197}\text{At}$ . Additionally, in these isotopes an isomeric state with a spin and parity of  $1/2^+$  ( $\pi s_{1/2}$ ) is observed [8,9]. The At nuclei are observed to become more deformed as the mass number is further decreased and the  $1/2^+$  state is observed to become the ground state at  $^{195}\text{At}$  [10,11]. These results are consistent with the measured changes of the mean-square charge radius, magnetic dipole, and spectroscopic quadrupole moments obtained with laser spectroscopy [12]. When moving towards the most exotic astatine nuclei, the pro-

duction cross sections are too low for  $\gamma$ -ray spectroscopy, and their half-lives become too short to permit studies with laser spectroscopy. However,  $\alpha$ -decay spectroscopy is an efficient technique to study these nuclei as only a few observations are enough to define the  $\alpha$ -particle energy  $E_\alpha$ , half-life  $T_{1/2}$ , mass-excess  $\Delta$ , and one proton separation energy  $S_p$ . The last two require prior knowledge of the mass excesses of the daughter nuclei, which, however, are often available from other sources. With the quantities above one can discuss fundamental questions, such as (i) the strength of shell closures, (ii) the location of the proton dripline, and (iii) the predictive power of atomic mass models. The  $\alpha$ -particle preformation factor and the overlap of the initial and final-state wave functions can be studied by calculating the reduced decay width  $\delta^2$  and the hindrance factor (HF). For example, in Ref. [13] the most neutron-deficient astatine isotope known to date,  $^{191}\text{At}$ , was studied via  $\alpha$ -decay spectroscopy.

In the present article an observation of a new isotope of astatine,  $^{190}\text{At}$ , is reported and its  $\alpha$ -decay properties are presented. The present data are used to address the fundamental questions (i)–(iii) as applicable. Although the odd-odd nuclei are generally speaking challenging to study, odd-odd bismuth, astatine, and francium nuclei have been observed to have a common feature. These nuclei often have a high-spin state ( $10^-$ ), low-spin state ( $3^+$ ), and occasionally there is observed to be a ( $7^+$ ) state; see, for example, Refs. [14–16]. The most neutron-deficient odd-odd astatine isotope before present study was  $^{192}\text{At}$  [17]. It was observed to have two  $\alpha$ -decaying states of which the longer-living ( $9^-$ ,  $10^-$ ) state was proposed to result from a  $[\pi 2f_{7/2} \otimes \nu 1i_{13/2}]$  configuration. However, in less neutron-deficient isotopes of bismuth and astatine this state is associated with a  $[\pi 1h_{9/2} \otimes \nu 1i_{13/2}]$  coupling.

### II. EXPERIMENTAL DETAILS

To produce  $^{190}\text{At}$  nuclei in the fusion-evaporation reaction  $^{109}\text{Ag}(^{84}\text{Sr}, 3n)^{190}\text{At}$ , a  $^{190}\text{At}$  target with a thickness

\*henna.e.kokkonen@jyu.fi

<sup>†</sup>Present address: iThemba LABS, Somerset West 7129, South Africa.

<sup>‡</sup>Present address: Radiation and Nuclear Safety Authority - STUK, Lähteentie 2, 96400 Rovaniemi, Finland.

<sup>§</sup>Present address: University of Helsinki, PL55, 00014 University of Helsinki, Finland.

<sup>||</sup>Present address: MTC Limited, Ansty Park, Coventry CV79JU, United Kingdom.

<sup>¶</sup>Present address: Radiation and Nuclear Safety Authority - STUK, Jokiniemenkuja 1, 01370 Vantaa, Finland.

TABLE I. The beam energies  $E_{\text{beam}}$ , the thickness of the carbon degrader foil  $d_c$  in front of the target, energy in the center of the target  $E_{\text{c.o.t.}}$ , and the irradiation times  $t$  used in this study.

$E_{\text{beam}}$ (MeV)	$d_c$ ( $\mu\text{g}/\text{cm}^2$ )	$E_{\text{c.o.t.}}$ (MeV)	$t$ (h)
380		367	38
380	200	356	22
390		377	89
390	100	372	32

of  $1 \text{ mg}/\text{cm}^2$  was irradiated with a  $^{84}\text{Sr}$  ion beam. Typical beam intensity was  $12 \text{ pnA}$ . The  $^{84}\text{Sr}$  ions were accelerated with the K-130 cyclotron at the Accelerator Laboratory of the University of Jyväskylä (JYFL). The used beam energies and other experimental conditions are listed in Table I. The gas-filled recoil separator RITU (Recoil Ion Transport Unit [18,19]) was used to select the fusion-evaporation residues, now called recoils, and to transport them to the focal plane of RITU. In the GREAT (Gamma Recoil Electron Alpha Tagging [20]) spectrometer at the focal plane the recoils passed through a multiwire proportional counter (MWPC) and were subsequently implanted into a double-sided silicon strip detector (DSSD) with a thickness of  $300 \mu\text{m}$ . To increase the DSSD area, there were two DSSDs side by side, each with 40 vertical and 60 horizontal strips with a strip width of 1 mm. The DSSD and MWPC were used to select recoils from the scattered beam and from the target-like particles by using their time-of-flight between the detectors and the energy loss of the particles in the MWPC. An event in the DSSD that did not generate a MWPC signal was considered as a decay. The calibration of the DSSD energy response was performed using well-known  $\alpha$  activities produced in  $^{78}\text{Kr} + ^{92}\text{Mo}$  reactions with an energy of  $E_{\text{beam}} = 365 \text{ MeV}$ . The  $\alpha$ -decaying isotopes used in the calibration were  $^{150}\text{Dy}$ ,  $^{163}\text{W}$ ,  $^{162}\text{W}$ ,  $^{167}\text{Os}$ ,  $^{166}\text{Os}$ , and  $^{167\text{m}}\text{Ir}$ . Data for each detector channel were collected and time stamped with a 100 MHz clock. The data were analyzed with the GRAIN [21] software package to track decay chains containing two or three consecutive decay events.

### III. RESULTS AND DISCUSSION

The events associated with  $^{190}\text{At}$  were selected using spatial and temporal correlations. The recoil-implantation event had to be followed by at least two  $\alpha$ -decay events in the same pixel of the DSSD to be considered as a decay of the new isotope. Additionally, the recoil implantation and the first  $\alpha$  decay must occur within 10 ms time window. The first and second  $\alpha$ -particle energies of such event chains are displayed in Fig. 1. One should notice that the correlation matrix is effectively free of randomly correlated background events around the marked  $^{190}\text{At}$  decay chains.

The  $^{190}\text{At}$   $\alpha$ -decay chains observed in this study are displayed in Fig. 2. Three different events of  $\alpha$ -decay were observed with an average  $\alpha$ -particle energy of  $E_\alpha = 7750(20) \text{ keV}$  and half-life  $T_{1/2} = 1.0_{-0.4}^{+1.4} \text{ ms}$ . Additionally, a fourth decay chain, starting with an escaping  $\alpha$  particle, was observed. The half-life was extracted with the Schmidt's maximum likelihood method [25], and the quoted  $\alpha$ -particle energy is the

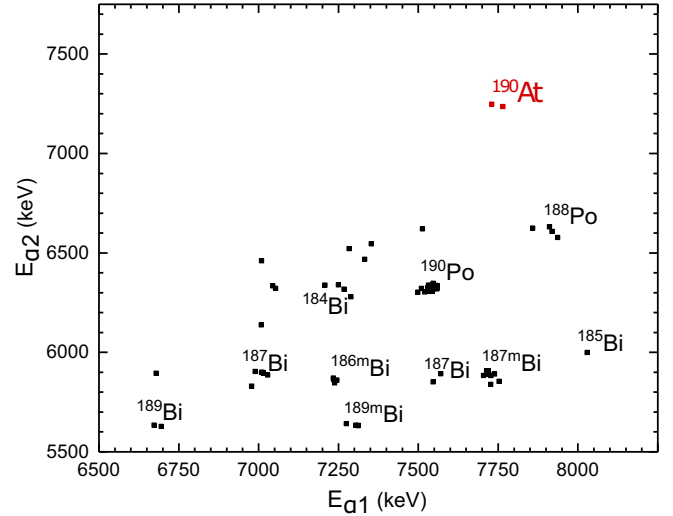


FIG. 1. The energies of the first two  $\alpha$  particles observed in the same pixel of the DSSD as the preceding recoil implantation event. The first decay must occur within 10 ms from the recoil implantation event. The previously known nuclei [22] are indicated with black.

arithmetic mean of the  $\alpha$ -particle energies of the individual full-energy events. In principle the recorded decay time of the escape event could be included in the half-life considerations, however, we leave this for the readers discretion. Additionally, the measured  $\alpha$ -particle energies are assumed to be free from  $\alpha$ -electron summing [26,27] since significantly more statistics would be required to address this effect in detail. The analysis using the Schmidt's radioactive decay probability test [28] was executed for the measured decay times. The decay times fit within the limits of the test and therefore the events are likely to originate from a decay of single radioactive species with a probability greater than 90%. Two of the events correlate with the  $^{186}\text{Bi}$  7263 keV  $\alpha$  particles. The full decay sequence is  $^{190}\text{At} \xrightarrow{\alpha} ^{186}\text{Bi} \xrightarrow{\alpha} ^{182}\text{Tl} \xrightarrow{\beta^+/EC} ^{182}\text{Hg} \xrightarrow{\alpha} ^{178}\text{Pt}$ . In practice the DSSD is insensitive to  $\beta^+$  decay and electron capture, therefore, the  $^{182}\text{Tl} \rightarrow ^{182}\text{Hg}$  step remains unobserved.

From the measured  $\alpha$ -particle energy, a  $Q_\alpha$  value of  $7920(20) \text{ keV}$  was calculated by assuming a ground state to ground state  $\alpha$  decay. In Fig. 3 the extracted  $Q_\alpha$  value is compared with those of other neutron-deficient astatine isotopes. The present value fits well to the systematics and therefore the possible deviation arising from this assumption is likely of the order of some tens of kilo electron volts, if any. In Fig. 3,  $Q_\alpha$  values predicted by selected mass models, the finite range droplet model (FRDM [29]), the shell model of Liran and Zeldes, and the average of six models based on different energy-density functionals (EDFs: SkP [30], SLy4 [31], SV-min [32], SkM\* [33], UNEDF0 [34], and UNEDF1 [35]) are also shown. The Mass Explorer interface [36] was used to obtain the EDF values. The present  $Q_\alpha$  value of  $^{190}\text{At}$  is best reproduced by the FRDM when considering the three selected mass models. Also, the EDF value is close to the measured value. However, it should be noted that the EDF data are unavailable for the most neutron-deficient odd-odd nuclei as indicated by the dashed lines. The model of

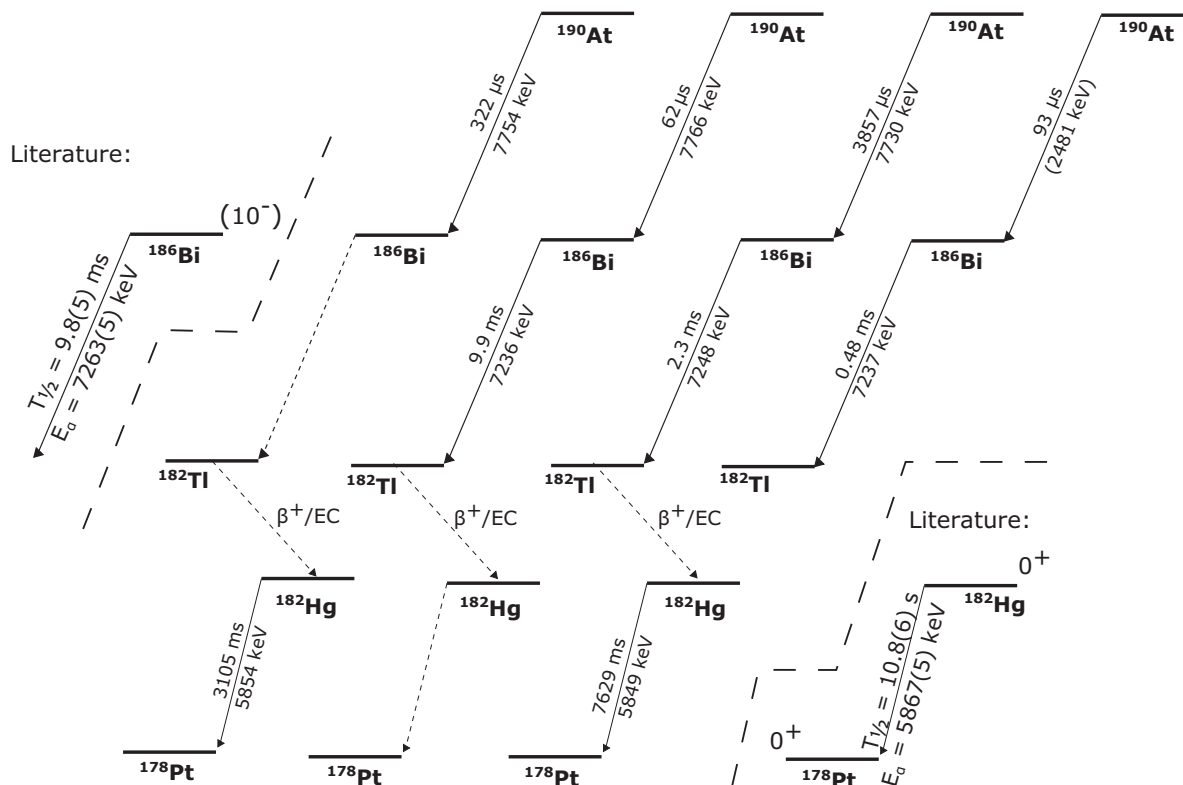


FIG. 2. The recorded decay data of the  $^{190}\text{At}$   $\alpha$ -decay chains observed in this study. The decays that were not observed are marked with a dashed line. Parentheses refer to escaped  $\alpha$  particle. The literature data are expressed above and below the thicker dashed lines [23,24].

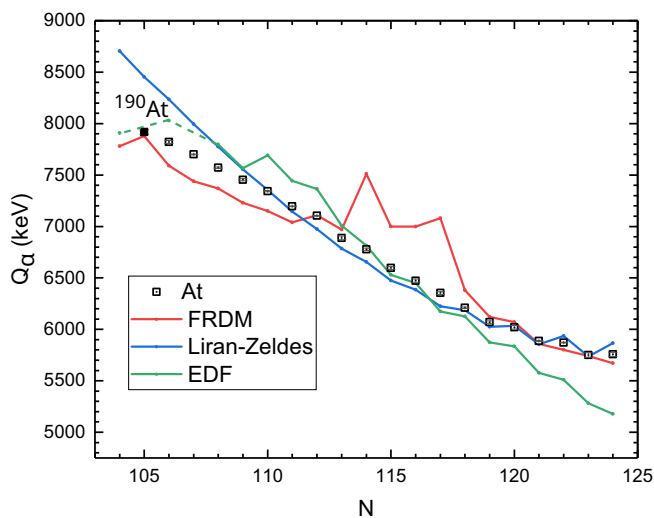


FIG. 3. Ground-state  $\alpha$ -decay energies  $Q_\alpha$  of atastine isotopes. The  $Q_\alpha$  value of  $^{190}\text{At}$  (neutron number 105) extracted in the present study is indicated by a solid symbol. The other experimental values, marked with open symbols, are from literature [41]. Solid lines are drawn through the values predicted by the mass models: FRDM(2012) [29], Liran-Zeldes [42], and EDFs (SkP [30], SLy4 [31], SV-min [32], SkM\* [33], UNEDF0 [34], and UNEDF1 [35]). The Mass Explorer interface [36] was used to obtain the EDF values. The EDF does not provide data for the most exotic odd-odd nuclei and therefore an interpolation is indicated with the dashed line.

Liran and Zeldes diverges from the measured values of the most exotic isotopes being still accurate for  $N \geq 109$  within  $\pm 200$  keV. The FRDM deviates from the measured values for  $N \approx 115$  isotopes significantly, but again reproduces the experimental values well closer ( $N \geq 118$ ) to the  $N = 126$  shell closure.

The reduced decay width and the  $\alpha$ -decay hindrance factor calculated by using the Rasmussen method [37] are  $\delta^2 = 70_{-50}^{+70}$  keV and  $HF = 1.0_{-0.5}^{+1.9}$ . These values were extracted using the half-life and the  $\alpha$ -particle energy of the present work, and by assuming a 100%  $\alpha$ -decay branch and an emission of  $s$ -wave  $\alpha$  particles. The  $HF$  was extracted by normalizing the  $\delta^2(^{190}\text{At})$  to that calculated from the  $\alpha$ -decay properties of  $^{212}\text{Po}$  [38]. As the theoretical prediction for the  $\beta$ -decay half-life is of the order of 600 ms [29], the  $\alpha$  decay is expected to dominate. The spin and parity of the daughter nucleus  $^{186}\text{Bi}$  has been proposed to be  $(10^-)$  based on the systematics [39]. As the obtained  $\alpha$ -decay hindrance factor is close to one, the initial and final states of the  $\alpha$  decay are likely to have the same spin and parity. Therefore, we suggest that the presently observed  $\alpha$ -decay activity is from a  $(10^-)$  state in  $^{190}\text{At}$ . In addition, fusion-evaporation reactions tend to favor feeding of high-spin states. Spin this high is possible to achieve only if the wave functions of the  $\alpha$ -decaying state involve Nilsson orbitals arising from  $\nu i_{13/2}$ ,  $\pi h_{9/2}$ , and  $\pi f_{7/2}$  spherical parentage.

The proton-decay energy for  $^{190}\text{At}$  has been predicted [40] to be higher than 1 MeV, thus it is interesting to consider whether the presently observed state could undergo proton

decay. The mass excess of the new isotope 7200(30) keV was extracted by using the presently determined  $Q_\alpha$  value, and mass excesses of the daughter nucleus and the  $\alpha$  particle,  $-3145(17)$  keV and  $2424.915\,87(15)$  keV, respectively [41]. The proton-decay energy of  $^{190}\text{At}$  can be deduced as the mass-excesses of the decay products  $^{189}\text{Po}$  [ $-1422(22)$  keV [41]] and proton [ $7288.971\,064(13)$  keV [41]] are known. The extracted proton-decay  $Q$  value is  $1330(40)$  keV. The partial half-life of a possible proton decay is approximated with a Wenzel-Kramers-Brillouin (WKB) integral by assuming that the proton is emitted from a  $h_{9/2}$  state. The resulting partial half-life for the proton decay is 30 s, therefore, the proton decay cannot compete with the  $\alpha$  decay. This fits with the fact that, despite the careful analysis, the proton decay remained unobserved in this experiment. A similar conclusion can be made if the emitted proton is assumed to occupy an  $f_{7/2}$  orbital as the calculated half-life is 90 ms. If an emission from a  $\pi s_{1/2}$  orbital is considered, the partial half-life is reduced to 2.5 ms, which is close to the measured  $\alpha$ -decay half-life. However, it should be noted that it is not possible to obtain ( $10^-$ ) state by any expected coupling of the  $s_{1/2}$  proton. The above-mentioned proton emission half-lives assume spherical nucleus which might be far-fetched. However, the quoted values can be taken as an order of magnitude estimate and thus can be used to assess whether the proton decay can compete with the  $\alpha$  decay.

#### IV. SUMMARY

A new exotic neutron-deficient isotope of astatine,  $^{190}\text{At}$ , was produced and identified. The isotope was produced using a fusion-evaporation reaction and studied by means of  $\alpha$ -decay spectroscopy at the focal plane of the gas-filled separator RITU. The measured  $\alpha$ -decay properties are an  $\alpha$ -particle energy and a half-life,  $7750(20)$  keV and  $1.0_{-0.4}^{+1.4}$  ms, respectively. The  $\alpha$  decay was concluded to be unhindered and therefore, a spin and parity of ( $10^-$ ) was proposed for the decaying state of  $^{190}\text{At}$ . Using the determined decay properties, the possibility of proton emission was considered. It was found to be unable to compete with the  $\alpha$  decay. The measured  $\alpha$ -decay properties were compared with the systematics and also predictions of the selected atomic mass models.

The data obtained in the present work and the corresponding metadata are available online [43].

#### ACKNOWLEDGMENTS

This work was supported by the Academy of Finland under the Contracts No. 323710, No. 347154, and No. 353786 (Personal research projects, K.A.). The contribution of M.V. was supported by the Slovak Research and Development Agency under Contract No. APVV-20-0532 and Slovak grant agency VEGA (Contract No. 2/0067/21).

- 
- [1] P. Möller, A. Sierk, R. Bengtsson, H. Sagawa, and T. Ichikawa, *At. Data Nucl. Data Tables* **98**, 149 (2012).
- [2] S. Hilaire and M. Girod, *Eur. Phys. J. A* **33**, 237 (2007).
- [3] S. Hilaire and M. Girod, AMEDEC database, [https://www-phynu.cea.fr/science\\_en\\_ligne/carte\\_potentiels\\_microscopiques/carte\\_potentiel\\_nucleaire\\_eng.htm](https://www-phynu.cea.fr/science_en_ligne/carte_potentiels_microscopiques/carte_potentiel_nucleaire_eng.htm).
- [4] T. P. Sjoreen, D. B. Fossan, U. Garg, A. Neskakis, A. R. Poletti, and E. K. Warburton, *Phys. Rev. C* **25**, 889 (1982).
- [5] K. Andgren, U. Jakobsson, B. Cederwall, J. Uusitalo, T. Bäck, S. J. Freeman, P. T. Greenlees, B. Hadinia, A. Hugues, A. Johnson, P. M. Jones, D. T. Joss, S. Juutinen, R. Julin, S. Ketelhut, A. Khaplanov, M. Leino, M. Nyman, R. D. Page, P. Rakhila *et al.*, *Phys. Rev. C* **78**, 044328 (2008).
- [6] K. Auranen, J. Uusitalo, S. Juutinen, U. Jakobsson, T. Grahn, P. T. Greenlees, K. Hauschild, A. Herzán, R. Julin, J. Konki, M. Leino, J. Pakarinen, J. Partanen, P. Peura, P. Rakhila, P. Ruotsalainen, M. Sandzelius, J. Sarén, C. Scholey, J. Sorri *et al.*, *Phys. Rev. C* **91**, 024324 (2015).
- [7] K. Auranen, J. Uusitalo, S. Juutinen, H. Badran, F. Defranchi Bisso, D. Cox, T. Grahn, P. T. Greenlees, A. Herzán, U. Jakobsson, R. Julin, J. Konki, M. Leino, A. Lightfoot, M. J. Mallaburn, O. Neuvonen, J. Pakarinen, P. Papadakis, J. Partanen, P. Rakhila *et al.*, *Phys. Rev. C* **97**, 024301 (2018).
- [8] K. Auranen, J. Uusitalo, S. Juutinen, U. Jakobsson, T. Grahn, P. T. Greenlees, K. Hauschild, A. Herzán, R. Julin, J. Konki, M. Leino, J. Pakarinen, J. Partanen, P. Peura, P. Rakhila, P. Ruotsalainen, M. Sandzelius, J. Sarén, C. Scholey, J. Sorri *et al.*, *Phys. Rev. C* **90**, 024310 (2014).
- [9] K. Auranen, J. Uusitalo, S. Juutinen, H. Badran, F. D. Bisso, D. Cox, T. Grahn, P. T. Greenlees, A. Herzán, U. Jakobsson, R. Julin, J. Konki, M. Leino, A. Lightfoot, M. Mallaburn, O. Neuvonen, J. Pakarinen, P. Papadakis, J. Partanen, P. Rakhila *et al.*, *Phys. Rev. C* **95**, 044311 (2017).
- [10] M. Nyman, S. Juutinen, I. Darby, S. Eeckhaudt, T. Grahn, P. T. Greenlees, U. Jakobsson, P. Jones, R. Julin, S. Ketelhut, H. Kettunen, M. Leino, P. Nieminen, P. Peura, P. Rakhila, J. Sarén, C. Scholey, J. Sorri, J. Uusitalo, and T. Enqvist, *Phys. Rev. C* **88**, 054320 (2013).
- [11] H. Kettunen, T. Enqvist, M. Leino, K. Eskola, P. Greenlees, K. Helariutta, P. Jones, R. Julin, S. Juutinen, H. Kankaanpää, H. Koivisto, P. Kuusiniemi, M. Muikku, P. Nieminen, P. Rakhila, and J. Uusitalo, *Eur. Phys. J. A* **16**, 457 (2003).
- [12] J. G. Cubiss, A. E. Barzakh, M. D. Seliverstov, A. N. Andreyev, B. Andel, S. Antalic, P. Ascher, D. Atanasov, D. Beck, J. Bieroń, K. Blaum, C. Borgmann, M. Breitenfeldt, L. Capponi, T. E. Cocolios, T. Day Goodacre, X. Derckx, H. De Witte, J. Elseviers, D. V. Fedorov *et al.*, *Phys. Rev. C* **97**, 054327 (2018).
- [13] H. Kettunen, T. Enqvist, T. Grahn, P. Greenlees, P. Jones, R. Julin, S. Juutinen, A. Keenan, P. Kuusiniemi, M. Leino, A.-P. Leppänen, P. Nieminen, J. Pakarinen, P. Rakhila, and J. Uusitalo, *Eur. Phys. J. A* **17**, 537 (2003).
- [14] M. Huyse, P. Decrock, P. Dendooven, G. Reusen, P. Van Duppen, and J. Wauters, *Phys. Rev. C* **46**, 1209 (1992).
- [15] P. Van Duppen, P. Decrock, P. Dendooven, M. Huyse, G. Reusen, and J. Wauters, *Nucl. Phys. A* **529**, 268 (1991).
- [16] J. Uusitalo, J. Sarén, S. Juutinen, M. Leino, S. Eeckhaudt, T. Grahn, P. T. Greenlees, U. Jakobsson, P. Jones, R. Julin, S. Ketelhut, A.-P. Leppänen, M. Nyman, J. Pakarinen, P. Rakhila, C. Scholey, A. Semchenkov, J. Sorri, A. Steer, and M. Venhart, *Phys. Rev. C* **87**, 064304 (2013).

- [17] A. N. Andreyev, S. Antalic, D. Ackermann, S. Franchoo, F. P. Heßberger, S. Hofmann, M. Huyse, I. Kojouharov, B. Kindler, P. Kuusiniemi, S. R. Leshner, B. Lommel, R. Mann, G. Münzenberg, K. Nishio, R. D. Page, J. J. Ressler, B. Streicher, S. Saro, B. Sulignano *et al.*, *Phys. Rev. C* **73**, 024317 (2006).
- [18] J. Sarén, J. Uusitalo, M. Leino, and J. Sorri, *Nucl. Instrum. Methods Phys. Res., Sect. A* **654**, 508 (2011).
- [19] M. Leino, J. Äystö, T. Enqvist, P. Heikkinen, A. Jokinen, M. Nurmia, A. Ostrowski, W. Trzaska, J. Uusitalo, K. Eskola, P. Armbruster, and V. Ninov, *Nucl. Instrum. Methods Phys. Res., Sect. B* **99**, 653 (1995).
- [20] R. Page, A. Andreyev, D. Appelbe, P. Butler, S. Freeman, P. Greenlees, R.-D. Herzberg, D. Jenkins, G. Jones, P. Jones, D. Joss, R. Julin, H. Kettunen, M. Leino, P. Rahkila, P. Regan, J. Simpson, J. Uusitalo, S. Vincent, and R. Wadsworth, *Nucl. Instrum. Methods Phys. Res., Sect. B* **204**, 634 (2003).
- [21] P. Rahkila, *Nucl. Instrum. Methods Phys. Res., Sect. A* **595**, 637 (2008).
- [22] Brookhaven National Laboratory, National Nuclear Data Center, <https://www.nndc.bnl.gov/>.
- [23] B. Singh and J. C. Roediger, *Nucl. Data Sheets* **111**, 2081 (2010).
- [24] E. Achterberg, O. Capurro, and G. Marti, *Nucl. Data Sheets* **110**, 1473 (2009).
- [25] K. H. Schmidt, C. C. Sahn, K. Pielenz, and H. G. Clerc, *Z. Phys. A: At. Nucl.* **316**, 19 (1984).
- [26] F. Hessberger, S. Hofmann, G. Münzenberg, K.-H. Schmidt, P. Armbruster, and R. Hingmann, *Nucl. Instrum. Methods Phys. Res., Sect. A* **274**, 522 (1989).
- [27] C. Theisen, A. Lopez-Martens, and C. Bonnafe, *Nucl. Instrum. Methods Phys. Res., Sect. A* **589**, 230 (2008).
- [28] K. Schmidt, *Eur. Phys. J. A* **8**, 141 (2000).
- [29] P. Möller, M. Mumpower, T. Kawano, and W. Myers, *At. Data Nucl. Data Tables* **125**, 1 (2019).
- [30] J. Dobaczewski, H. Flocard, and J. Treiner, *Nucl. Phys. A* **422**, 103 (1984).
- [31] E. Chabanat, P. Bonche, P. Haensel, J. Meyer, and R. Schaeffer, *Nucl. Phys. A* **635**, 231 (1998).
- [32] P. Klüpfel, P.-G. Reinhard, T. J. Bürvenich, and J. A. Maruhn, *Phys. Rev. C* **79**, 034310 (2009).
- [33] J. Bartel, P. Quentin, M. Brack, C. Guet, and H.-B. Håkansson, *Nucl. Phys. A* **386**, 79 (1982).
- [34] M. Kortelainen, T. Lesinski, J. Moré, W. Nazarewicz, J. Sarich, N. Schunck, M. V. Stoitsov, and S. Wild, *Phys. Rev. C* **82**, 024313 (2010).
- [35] M. Kortelainen, J. McDonnell, W. Nazarewicz, P.-G. Reinhard, J. Sarich, N. Schunck, M. V. Stoitsov, and S. M. Wild, *Phys. Rev. C* **85**, 024304 (2012).
- [36] Michigan State University, Mass Explorer interface, <http://massexplorer.frib.msu.edu/>.
- [37] J. O. Rasmussen, *Phys. Rev.* **113**, 1593 (1959).
- [38] K. Auranen and E. McCutchan, *Nucl. Data Sheets* **168**, 117 (2020).
- [39] C. M. Baglin, *Nucl. Data Sheets* **99**, 1 (2003).
- [40] X. Yin, R. Shou, and Y. M. Zhao, *Phys. Rev. C* **105**, 064304 (2022).
- [41] M. Wang, W. Huang, F. Kondev, G. Audi, and S. Naimi, *Chin. Phys. C* **45**, 030003 (2021).
- [42] S. Liran and N. Zeldes, *At. Data Nucl. Data Tables* **17**, 431 (1976).
- [43] <https://doi.org/10.23729/0a9fb1a9-c0e8-4f4d-8976-148cb1ef4c6a>.